Experimental Parasitology 135 (2013) 532–540

Contents lists available at ScienceDirect

Experimental Parasitology

journal homepage: www.elsevier.com/locate/yexpr

Entamoeba histolytica P-glycoprotein (EhPgp) inhibition, induce trophozoite acidification and enhance programmed cell death

Olivia Medel Flores [a], Consuelo Gómez García [a], Virgina Sánchez Monroy [a,c], José D' Artagnan Villalba Magadaleno [d], Elvira Nader García [a], D. Guillermo Pérez Ishiwara [a,b,*]

[a] Programa Institucional de Biomedicina Molecular ENMyH, Instituto Politécnico Nacional, Guillermo Massieu Helguera No. 239, CP 07320, México DF, Mexico
[b] Centro de Investigación en Biotecnología Aplicada (CIBA), Instituto Politécnico Nacional, Ex-Hacienda San Juan Molino Carretera Estatal Tecuexcomac-Tepetitla Km 1.5, Tlaxcala CP 90700, Mexico
[c] Escuela Militar de Graduados de Sanidad, UDEFA, CP 11620, Mexico
[d] Escuela Médico Militar, UDEFA, CP 11620, Mexico

HIGHLIGHTS

- Overexpression of anti-Pgp5 transcript diminished P-glycoprotein expression.
- Inhibition of PGP produced acidification of intracellular pH.
- PGP overexpression prevent intracellular acidification and PCD.

GRAPHICAL ABSTRACT

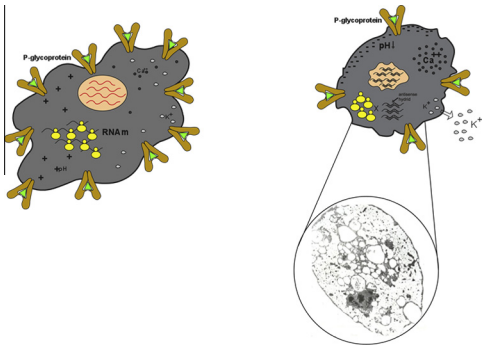

ARTICLE INFO

Article history:
Received 6 November 2012
Received in revised form 15 August 2013
Accepted 25 August 2013
Available online 5 September 2013

ABSTRACT

Programmed cell death (PCD) is induced in *Entamoeba histolytica* by a variety of stimuli *in vitro* and *in vivo*. In mammals, intracellular acidification serves as a global switch for inactivating cellular processes and initiates molecular mechanisms implicated in the destruction of the genome. In contrast, intracellular alkalinization produced by P-glycoprotein overexpression in multidrug-resistant cells has been related to apoptosis resistance. Our previous studies showed that overexpression of *E. histolytica* P-glycoprotein (PGP) altered chloride-dependent currents and triggered trophozoite swelling, the reverse process of cell shrinkage produced during PCD. Here we showed that antisense inhibition of PGP expression produced a synchronous death of trophozoites and the enhancement of biochemical and morphological characteristics of PCD induced by G418. The nucleus was contracted, and the nuclear membrane was disrupted. Moreover, chromatin was extensively fragmented. Ca^{2+} concentration was increased, while the intracellular pH ($_i$pH) was acidified. In contrast, PGP overexpression prevented intracellular acidification and circumvented the apoptotic effect of G418.

* Corresponding author at: Programa Institucional de Biomedicina Molecular ENMyH, Instituto Politécnico Nacional, Guillermo Massieu Helguera No. 239, CP 07320, México DF, México. Fax: +52 57 29 63 00x55534.
E-mail addresses: ishiwaramx@yahoo.com.mx, dperez@ipn.mx (D.G. Pérez Ishiwara).

0014-4894/$ - see front matter © 2013 Elsevier Inc. All rights reserved.
http://dx.doi.org/10.1016/j.exppara.2013.08.017

1. Introduction

Amoebiasis produced by *Entamoeba histolytica* is a major public health disease in developing countries. It affects 500 million people, and each year causes 50 million clinical cases of dysentery or amoebic liver abscess along with 100,000 deaths (World Health Organization, 1997). Reports on drug treatment failure and the generation of drug-resistant clones *in vitro* suggest that drug resistance might be clinically important in the near future (Hanna et al., 2000; Wassmann et al., 1999; Samarawickrema et al., 1997). Although the overexpression of P-glycoproteins (PGPs) has been implicated in the development of the multidrug-resistance phenotype (MDR) (Jonstone et al., 2000; Tsai et al., 2007), a large body of evidence strongly supports important roles for PGPs that only to extrude chemotherapeutic agents from cells (Ambudkar et al., 1999; Borst et al., 1999; Gottesman and Pastan, 1993; Sharom et al., 1993).

PGPs have been implicated in the removal of xenobiotic agents from the cell, lipid metabolism and translocation (Cordon-Cardo et al., 1989; van Helvoort et al., 1996; Jonstone et al., 2000), as well as cytokine transport (Drach et al., 1996), PGPs are also potential regulators of ion channels and cell swelling-activated chloride channels (Valverde et al., 1996; Delgadillo et al., 2002).

Previous reports have proposed that PGP overexpression also confers resistance to apoptosis (Robinson et al., 1997). Apoptosis is an active and energy-dependent process characterized in part by nuclear condensation and cell shrinkage (Perl et al., 2005). It has been evolutionarily conserved for most animal and plant species, but presents inter- and intra-species variations. It has been partially described in various parasites, such as *Leishmania*, (Holzmuller et al., 2002) *Trichomonas* (Chose et al., 2002) and *Trypanosoma* (De souza et al., 2006).

Recently, our group (Villalba et al., 2007a) and others (Ghosh et al., 2010; Ramos et al., 2007) reported that programmed cell death (PCD) is induced in *E. histolytica* by G-418 antibiotic, nitric oxide and oxygen reactive species. The process is characterized by cell shrinkage, DNA fragmentation, overproduction of reactive oxygen species (ROS), intracellular pH acidification, decreased intracellular K^+ and increased cytosolic calcium (Villalba et al., 2007a; Ghosh et al., 2010). Ramos et al., (2007) found that PCD is also marked by the inhibition of hemolytic activity and complement resistance, which suggested that molecules, such as phospholipases, amoebapores and CD59, are affected. Several cellular markers of PCD have been defined; Meisenholder et al., 1996 proposed that intracellular acidification serves as a global switch to inactivate cellular processes and initiate the molecular mechanisms implicated in the destruction of the genome. In contrast, other studies suggested that overexpression of P-glycoprotein in multidrug-resistant cells is related to apoptosis resistance (Robinson et al., 1997), and it has also been associated with intracellular alkalinization (Robinson et al., 1997). In concordance with these results, our previous reports in *E. histolytica* demonstrated that EhPGP5 overexpression alters chloride-dependent currents and causes trophozoite swelling (Delgadillo et al., 2002; Bañuelos et al., 2002), the reverse process of cell shrinkage reported during the induction of PCD (Nickel and Tannich, 1994). Whether or not intracellular alkalinization triggered by P-glycoproteins overexpression prevents apoptotic acidification and other aspects of the apoptosis cascade is still unknown. In this study, we showed that inhibition of *E. histolytica* P-glycoprotein produced the acidification of intracellular pH ($_i$pH) and enhancement of PCD induced by G418. In contrast, PGP overexpression prevented intracellular acidification and circumvented the PCD.

2. Materials and methods

2.1. E. histolytica trophozoites

Clone CA trophozoites (strain HM1: IMSS) were axenically cultured in TYI-S-33 medium (Diamond et al., 1978). Transfected trophozoites were cultured in the presence of 10 μg/ml of G418.

2.2. EhPgp5 and anti-EhPgp5 plasmid constructions

The complete *EhPgp5* was cloned in the transcription vector pBS-KS (Stragene, CA) under the T7 promoter direction (pBSEhPgp5) using the *KpnI* and *BamHI* enzymes. PCR amplifications were performed with pBSEhPgp5 plasmid (50 ng) as template, 2.5 U of Taq polymerase (Qiagen) and the following primer sets: Pgp5 S-25 (5′ AAGGATCCATGACAAGTGAACCAGC 3′) and Pgp5 AS-25 (5′ TTGGTACCTTAATTCACAGTTCCAA 3′) for the *EhPgp5* complete open reading frame (ORF) (3900 bp); and antiS-28 (5′ GTAGGAGGTGCAGTATTCCC 3′) and antiAS-29 (5′ GTCAAACAAGAAATAGGATGG 3′) aligning in the positions 2158 and 2428 of the ORF, respectively to amplified a 270 bp *EhPgp5* antisense fragment. PCR was performed using the following profile for 30 cycles: 94 °C for 50 s, 47 °C for 40 s and 72 °C for 3.5 min, according to standard methods. PCR products were cloned independently into the TA one-step cloning vector (Invitrogen) and subcloned into the transfection vector pEhNeoCAT (kindly provided by Dr. E. Tannich, Hamburg, Germany). The CAT gene was replaced by cloning the *EhPgp5* ORF or the *EhPgp5* antisense sequence into the *KpnI*/*BamHI* sites to generate the pNeoEhPgp5 and pNeoAnti-EhPgp5 plasmids.

2.3. Transfection assays

Clone CA trophozoites (1×10^6) were transfected with 250 μg pNeoEhPgp5 or pNeoAnti-EhPgp5 plasmids as described (Nickel and Tannich, 1994). Plasmid containing only the neomycin gene (pNeo) was used as control. Electroporated trophozoites were incubated in TYI-S-33 medium for 48 h at 37 °C. Cultures were selected with G418 (10 μg/ml) to generate the CANeo, CANeoPgp5 and CANeoAnti-Pgp5 clones.

2.4. Kinetics of growth

After transfection, CANeo, CANeoPgP5 or CANeoAnti-Pgp5 clones (1×10^5 trophozoites) were grown in the presence of G418 (10 μg/ml). Cell counting was evaluated every 12 h during 72 h. Viability of trophozoites was determined by trypan blue dye exclusion using an inverted microscope (Nikon Eclipse TE-300) and a Neubauer chamber. Transfections were done in three independent biological replicates.

2.5. Detection of EhPgp5, anti-EhPgp5 and Neo transcripts by reverse transcriptase-polymerase chain reaction (RT-PCR)

Total RNA was isolated with Trizol reagent according to the manufacturer's protocol (Invitrogen). RNA concentration was determined spectrophotometrically at 260 nm. Isolated RNA was treated with RQ1 RNase-Free DNase (Promega) to avoid genomic DNA contamination. RNAs (5 μg) from CANeo, CANeoPgP5 or CANeoAnti-Pgp5 clones obtained after 12 h of 10 μg/ml G418 incubation, were reverse transcribed with a Access RT-PCR System Kit (Promega), containing 10 mM dNTPs, AMV/TFI buffer, 25 mM $MgSO_4$, 5 U of AMV reverse transcriptase (Promega) and 40 μM each of antisense oligonucleotides (Pgp5 AS-25 and antiAS-29). The ASNeo oligonucleotide (5′ TTAGAAGAACTCGTC 3′) was used for *Neo* synthesis. The reactions were incubated at 48 °C for

45 min. For the PCR protocol, we added in three independent reactions Taq DNA polymerase (Promega) and the Pgp5S-25, antiS-28 or SNeo sense oligonucleotides. PCRs were performed in a Perkin-Elmer thermal cycler for 30 cycles (94 °C for 30 s, 47 °C for 35 s, 72 °C for 38 s) with a final extension step of 72 °C for 7 min. Amplified fragments of 270 bp for *EhPgp5* and *anti-EhPgp5* and 700 bp for *Neo* were obtained and analyzed in 2% agarose gels stained with ethidium bromide solution (0.5 μg/ml; Gibco).

2.6. Quantitative real-time PCR (qRT-PCR) assays

The inhibition of *EhPgp5* expression was evaluated by triplicate in three independent biological replicates. Total RNA from CANeo, CANeoPgP5, or CANeoAnti-Pgp5 clones obtained after 12 h of 10 μg/ml G418 incubation, were isolated, quantified, and treated with DNase. RNAs were reverse transcribed using the Cloned AMV First Strand cDNA Synthesis Kit (Invitrogen), according to the manufacturer's protocol. Quantitative RT-PCRs (qRT-PCRs) were performed by real-time monitoring of fluorescence in the ABI PRISM 7000 Sequence Detection System (Applied Biosystems) using the primers for *EhPgp5* and the SYBR Green PCR Master Mix (Applied Biosystems, Foster, CA). *GAPDH* (glyceraldehyde 3-phosphate dehydrogenase) was used as an internal control.

Relative quantification was calculated by the comparative Cycle Threshold (CT) method, which uses the arithmetic formula $2^{-\Delta\Delta CT}$ (Livak and Schmittgen, 2001). To validate the $2^{-\Delta\Delta CT}$ method, we verified that the amplification efficiency of *EhPgp* gene and the internal control *GAPDH* were nearly equal. Statistically significant differences in gene expression between transfected and non-transfected trophozoites after 12 h of G418 incubation were analyzed using Kruskal–Wallis One-Way Analysis of Variance on Ranks (Livak and Schmittgen, 2001) and multiple comparisons were analyzed with the Tukey Test.

2.7. Western blot assays

Cell lysates of CANeo, CANeoPgp5 and CANeoAnti-Pgp5 trophozoites incubated for 12 h in the presence of 10 μg/ml G418 were prepared after three freeze–thaw cycles in 100 mM *p*-hydroxymercuribenzoic acid (PHMB) (Sigma). Total extracts (50 μg) from each clone were analyzed by 7.5% SDS–PAGE and transferred to nitrocellulose membranes (Amersham, Biosciences). Western blot assays were performed with anti-EhPgp384 antibody (1:2000 dilution) (Bañuelos et al., 2002). Nitrocellulose membranes were incubated with horseradish peroxidase (HRP)-conjugated goat anti-rabbit immunoglobulin G (IgG; Zymed; 1:1000) for 1 h. Antigen–Antibody reactions were revealed with a fresh preparation of 3 mg/ml of 4-choro-1-naphtol until the color was developed. For internal control, membranes were incubated with monoclonal mouse anti-actin antibody (1:1000; kindly provided by Dr. Manuel Hernández, CINVESTAV, México) and HRP-conjugated anti-mouse IgG antibody (Zymed; 1:2000). Western blot experiments were done by triplicate.

2.8. Terminal dUTP nick end labeling (TUNEL)

CA, CANeo, CANeoPgp5 and CANeoAnti-Pgp5 clones were incubated with G418 (10 μg/ml) for 12 h. Trophozoites were fixed in 4% formaldehyde for 45 min at 4 °C. After two PBS washes, 50 μl of TUNEL reaction mixture of the *In situ* cell death detection kit (Roche) was added and incubated for 60 min at 37 °C in a humidified atmosphere in the dark. Slides were rinsed 3 times with PBS and visualized with a Nikon fluorescence microscope. As a negative control, clone CA trophozoites were grown without G418. As an internal control, trophozoites were incubated with *DNAse I* (Promega).

2.9. Transmission electron microscopy

Trophozoites of clones CA, CANeo, CANeoPgP5 and CANeoAnti-PgP5 were incubated for 12 h in the presence of G418 (10 μg/ml) and washed twice with 0.1 M sodium cacodylate buffer, pH 7.4. Cells were fixed for 1 h with 2.5% glutaraldehyde in 0.1 M sodium cacodylate buffer, pH 7.4. Fixed trophozoites were washed twice with 0.1 M sodium cacodylate buffer, post-fixed with 2% osmium tetroxide, dehydrated with increasing concentrations of ethanol and treated with propylene oxide. Trophozoites were then embedded in epoxy resins. Semi-thin sections were stained with toluidine blue for examination by light microscopy. Thin sections were stained with uranyl acetate, followed by lead citrate, and then examined in a Zeiss EM-10 electron microscope.

2.10. Flow cytometry assay

Changes in the size and light scattering properties of trophozoites were determined by flow cytometry, as described by Hawley in 2004, with a Becton Dickinson FACSCalibur equipped with Cell Quest software (Becton Dickinson). CA, CANeo, CANeoPgp5, and CANeoAnti-Pgp5 trophozoites (1×10^6) were treated with G418 (10 μg/ml) for 12 h and analyzed with a 488 nm argon laser. A specific gate, based on the proprieties of control trophozoites, was selected to determine position identifications on a forward scatter versus side scatter dot plot. Light scattered in the forward direction is roughly proportional to cell size, whereas light scattered at a 90° angle (side scatter) is proportional to cell density.

2.11. Cytosolic Ca^{2+} concentrations

Changes in intracellular Ca^{2+} concentration ($_i[Ca^{2+}]$) were monitored in CA, CANeo, CANeoPgp5 and CANeoAnti-Pgp5 clones using the fluorescent probe Fura-2/AM (Sigma) after 140 min of incubation with G418 (10 μg/ml). Trophozoites (1×10^6) were washed twice at 1500 rpm for 2 min at 4 °C in buffer I (116 mM NaCl, 5.4 mM KCl, 0.8 mM $MgSO_4$, 5.5 mM D-glucose, and 50 mM HEPES, pH 7.0). Amoebae were resuspended in loading buffer (116 mM NaCl, 5.4 mM KCl, 0.8 mM $MgSO_4$, 5.5 mM D-glucose, 1.5% sucrose, 50 mM HEPES, pH 7.4, and 6 μM Fura-2/AM). The cellular suspension was incubated for 1 h at 37 °C with soft agitation. Trophozoites were washed four times with ice-cold buffer I to remove extracellular dye. For fluorescence measurements, 125 μl of trophozoite suspension was diluted with 2.4 ml of buffer I. Fura-2/AM was excited at 340 nm, and emission at 510 nm was registered by a Perkin Elmer MPF44A fluorimeter. The $_i[Ca^{2+}]$ concentrations were determined at 30 °C using the formula:

$$i[Ca^{2+}] = Kd \times \frac{(F2 - F3)}{(F4 - F1)} \text{nmoles}$$

*F*1 is the fluorescence signal obtained from the entire cell, while *F*2 represents the fluorescence signal after addition of 1 mM EGTA. *F*3 is the fluorescence following cell lysis with 0.04% Triton X-100 in 30 mM Trizma base, and *F*4 is the fluorescence after adding 4 mM CaCl2. *Kd* represents the dissociation constant value of 224 nM, as reported (Grynkiewicz et al., 1985).

2.12. Intracellular $_ipH$ measurements

Trophozoites (1×10^6) of CANeo, CANeoPgP5, and CANeoAnti-PgP5 clones were incubated with G418 (10 μg/ml) for 12 h, resuspended in TYI-S-33 medium and washed twice with buffer A (140 mM KCl, 4 mM $CaCl_2$, 25 mM HEPES-Tris, pH 7.4). Trophozoites were then loaded with 10 μM 2,7-bis (2-carboxyethyl)-5-(and 6)-carboxyfluorescein (BCECF) (Sigma) for 45 min in 1 ml

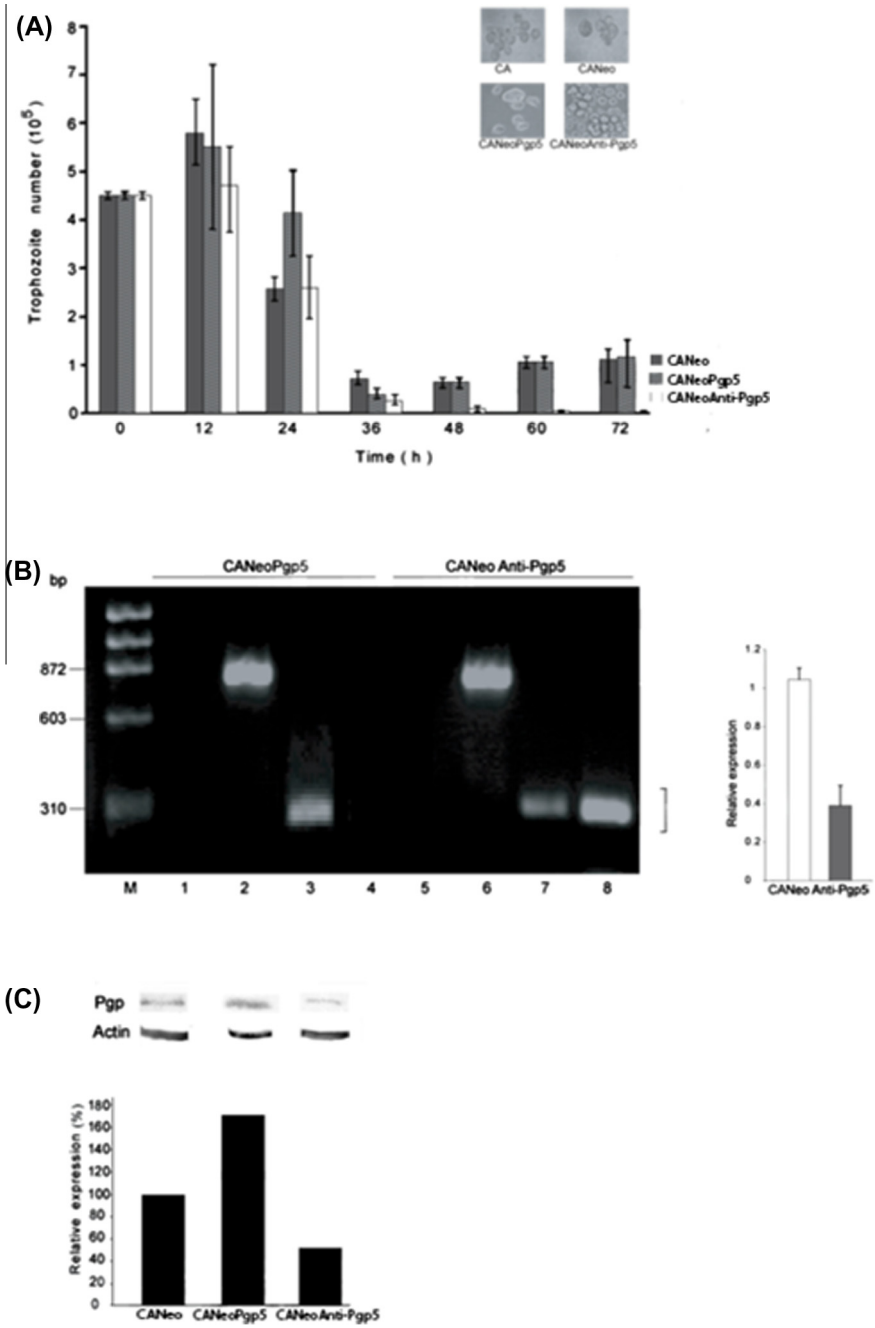

Fig. 1. Viability and PGP expression in CANeoAnti-Pgp5 trophozoites. (A) Kinetics of growth of CANeo, CANeoPgp5 and CANeoAnti-Pgp5 trophozoites cultured in the presence of G418. Viability was evaluated every 12 h by trypan blue exclusion. Upper panel shows trophozoite morphology at 12 h. (B) Left, agarose gel (2%) electrophoretic mobility of RT-PCR products using 5 μg/μl of total RNA from CANeoPgp5 and CANeoAnti-Pgp5 trophozoites incubated with 10 μg/ml G418 antibiotic after 12 h. Lane M, φX174DNA/*Hae* III molecular marker; lanes 2 and 6, lanes 3 and 7, and lanes 4 and 8 show *Neo*, *EhPgp5* and *anti-EhPgp5* RT-PCR transcription products, respectively. Lanes 1 and 5 are the negative controls. Right, relative expression of *EhPgp5* gene in CANeoAnti-Pgp5 clone grown without G418 (empty bar graph) or in the presence of G418 after 12 h of incubation (fill bar graph) (10 μg/ml). (C) Western-blot analysis showing EhPgp5 protein expression (anti-EhPgp384 antibody) in CANeo, CANeoPgp5 and CANeoAnti-Pgp5. Anti-actin antibody was used as an internal control. The graph shows the densitometry analysis of P-glycoprotein expression levels, using the actin detection for normalization.

buffer A, supplemented with nigericin (1 μg/ml). Finally, fluorescence was registered at 535 nm in a Perkin Elmer MPF44A fluorimeter.

3. Results

3.1. Establishment of trophozoites transfected with EhPgp5 and anti-EhPgp5 sequences

Trophozoites transfected with pNeoEhPgp5 (CANeoPgp5) and pNeoAnti-EhPgp5 (CANeoAnti-Pgp5) were selected using G418 (10 μg/ml). Fig. 1A shows the growth kinetics of both test clones and the control CANeo clone. While trophozoites transfected with pNeo or pNeoEhPgp5 plasmids were able to grow after 48 h of G418 selection, no stable transfectants were obtained with the pNeoAnti-Pgp5 plasmid. At the beginning of incubation (12 h), CANeoAnti-EhPgp5 trophozoites had rounded forms, and cell shrinkage was evident (upper panel). Trophozoite death was observed after 24 h of G418 treatment. Multiple transfection assays with lower amounts of the selection antibiotic or higher plasmid concentrations were performed without any success. To ascertain

if the CANeoAnti-Pgp5 trophozoites expressed the *Neo* resistance gene and to determine if there was any relationship between the incapability of trophozoites to grow in the presence of G418 with overexpression of *anti-EhPgp5*, trophozoites from each clone were collected after 12 h of G418 incubation to perform RT-PCR and Western blot assays. Fig. 1B demonstrates that the *Neo* transcript was similarly detected in CANeoPgp5 and CANeoanti-Pgp5 trophozoites (Fig. 1B, lanes 2 and 6). The Pgp5 transcript, as expected, was overexpressed in CANeoPgp5 (Fig. 1B, lane 3). Detection was lower in CANeoAnti-Pgp5 probably due to basal expression of P-glycoprotein in trophozoites (Fig. 1B, lane 7). In contrast, *anti-EhPgp5* transcript was not detected in CANeoPgp5 (Fig. 1B, lane 4), while it was strongly expressed in CANeoAnti-Pgp5 trophozoites (Fig. 1B, lane 8). Negative RT-PCR controls using RNAs as templates from both clones are shown in lanes 1 and 5. Quantitative real-time expression analysis of CANeoAnti-Pgp5 trophozoites showed that after 12 h incubation with G418 (10 μg/ml), *EhPgp5* gene expression diminished 60% of levels displayed in the absence of drug (Fig. 1B, graph).

Densitometry analysis of Western blot assays (Fig. 1C) revealed that trophozoites of clone A transfected with the Neo plasmid (CANeo) displayed a basal P-glycoprotein expression, in concordance with the expression of the wild type (CA) trophozoites (Bañuelos et al., 2002). In contrast, trophozoites of CANeoPgp5 showed an increment of 71% from the basal P-glycoprotein expression after 12 h of G418 incubation. Interestingly, the P-glycoprotein expression diminished significantly in trophozoites expressing the antisense sequence (CANeoAnti-Pgp5), representing only the 54.3% of the CANeo expression. These results suggested that overexpression of the antisense Pgp5 sequence could interfere with P-glycoprotein production. Actin was used as an internal control.

3.2. Anti-EhPgp5 transcript overexpression altered nuclear structure and DNA

We previously detected DNA fragmentation during PCD induction with TUNEL staining (Villalba et al., 2007a). To investigate if *anti-EhPgp5* transcript overexpression was associated with trophozoite death, we assayed positive TUNEL staining in CANeoAnti-Pgp5 trophozoites in comparison to trophozoites from CA, CANeo and CANeoPgp5 clones. Fig. 2A shows that parasites expressing the *Neo* gene or the *Neo* and *EhPgp5* genes (CANeo and CANeoPgp5, respectively) displayed few positive staining nuclei. In contrast after G418 incubation, non-transfected trophozoites (CA) and trophozoites overexpressing the *anti-EhPgp5* sequence (CANeoAnti-Pgp5) showed several positive staining nuclei (Fig. 2A). As a positive control, trophozoites were incubated with *DNAse I* endonuclease and a negative staining control was also performed.

We further analyzed the ultrastructural changes associated with nuclear shrinkage, chromatin condensation and DNA fragmentation. Using transmission electron microscopy (Fig. 2B), we found that non-G418-treated trophozoites from the different clones had dense peripheral chromatin with a central endosome, while the nuclear and plasma membranes appeared intact (Fig. 2B, left panels). After 12 h of G418 incubation (Fig. 2B, right panels), the clones displayed important differences. Chromatin in CA trophozoites appeared fragmented and displaced to one side of the amoeba nucleus with round nuclear bodies and several glycogen deposits in the cytoplasm. CANeo and CANeoPgp5 trophozoite clones did not show any alterations; chromatin remained peripheral, and the nuclei appeared normal. However, the ultrastructural architecture of CANeoAnti-Pgp5 trophozoites presented several alterations. The cytoplasm showed abundant vacuoles and glycogen deposits. The nuclear membrane was not clearly defined, and the DNA seems to be damage (inset of CANeoAnti-Pgp5, Fig. 2B). Moreover, chromatin was fragmented, and several small nuclear bodies were evident; the cytoplasmic membrane remained integrate.

3.3. Cellular and biochemical changes associated with PCD

In *E. histolytica*, we had previously reported that PCD produced cytoplasmic alterations as a consequence of cell damage. To ascertain whether death produced in trophozoites transfected with

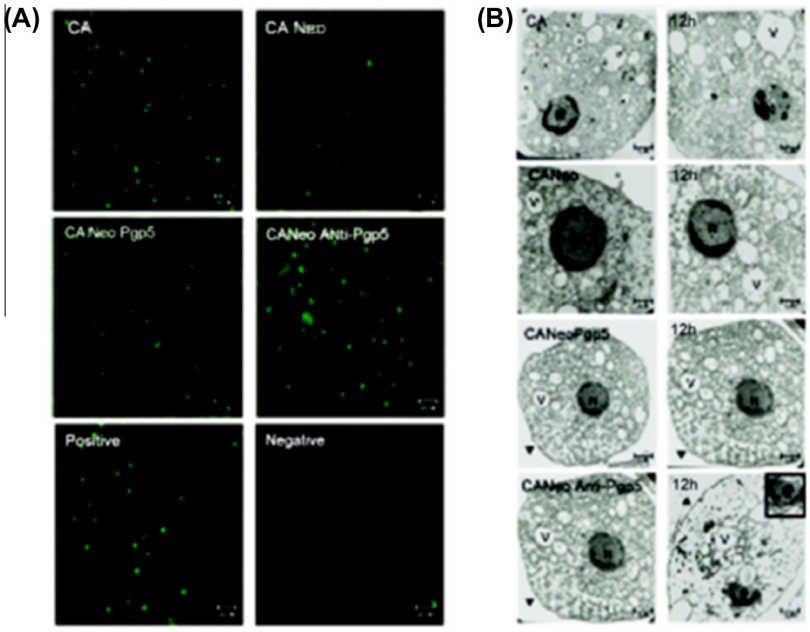

Fig. 2. DNA fragmentation and ultrastructural changes in trophozoites after G418 treatment. (A) Confocal microscopy analysis showing nuclear TUNEL staining of CA, CANeo, CANeoPgp5 and CANeoAnti-Pgp5 trophozoites after treatment with G418 (10 μg/ml). As a positive control, trophozoites were treated with *DNase I*; negative control is also shown. Bars, 20 μm. (B) Ultrastructure of CA, CANeo, CANeoPgp5 and CANeoAnti-Pgp5 trophozoites before (left panels) and after (right panels) G418 treatment. (N), nucleus; (V) vacuoles. Arrows show the plasma membrane. Inset in CANeoAnti-Pgp5 (12 h) showed the nuclear damage.

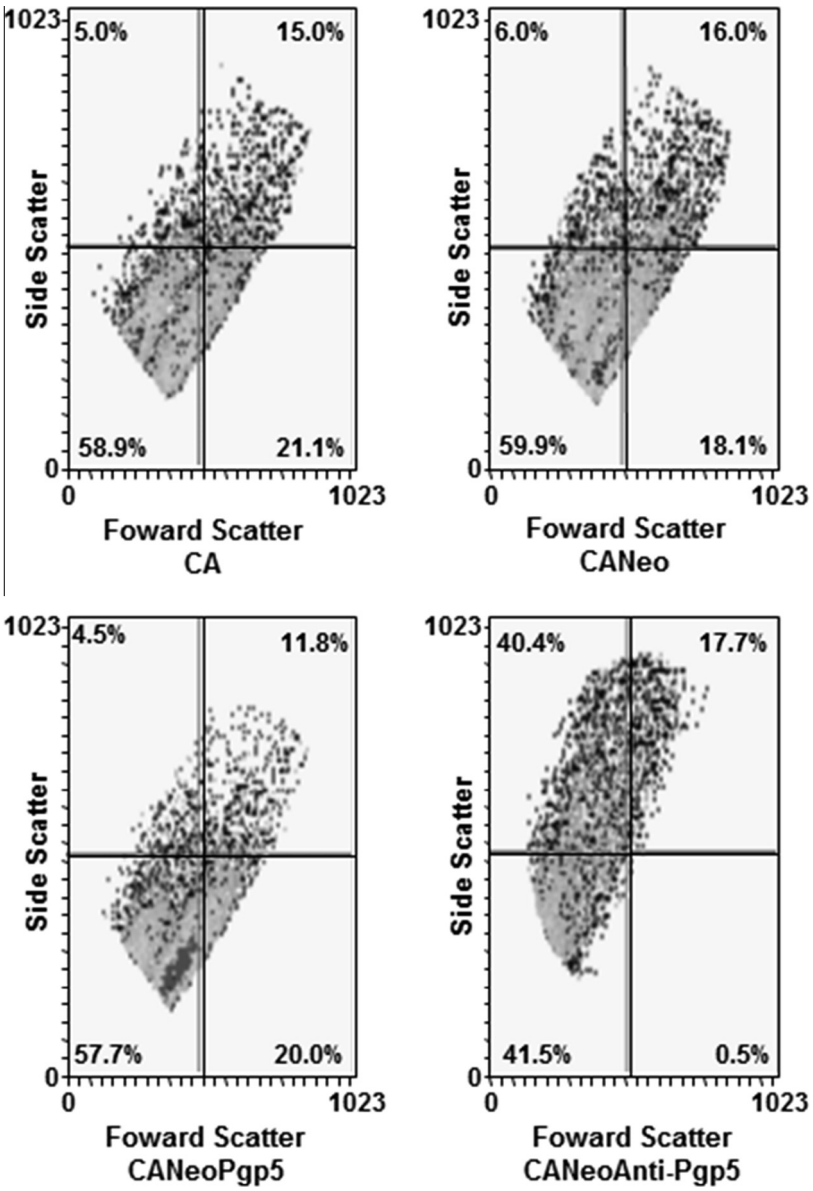

Fig. 3. Cell size and granularity of trophozoites after G418 treatment. Representative flow cytometry plots indicate cell size (forward scatter) and granularity (side scatter) of CANeo, CANeoPgp5 and CANeoAnti-Pgp5 trophozoites that were cultured in the presence of G418 (10 μg/ml). CA plot of trophozoites grown without drugs was utilized as a control.

antisense construct had the typical morphological and biochemical changes associated with PCD, we measured cell size and granularity. Fig. 3 demonstrates that the CANeoAnti-Pgp5 trophozoite population displayed a substantial reduction in cell size. While the population sizes of trophozoites from CA, CANeo and CANeoPgp5 (36%, 34% or 32%, respectively) were greater than the mean value. Trophozoites expressing the *anti-EhPgp5* sequence had diminished size; only 18% of the trophozoites were over the mean x axis value. The results in the side scatter plot suggested a dramatic increase in granularity in the CANeoAnti-Pgp5 trophozoites; 20%, 22% and 16% in CA, CANeo and CANeoPgp5, respectively, compared to 58% in CANeoAnti-Pgp5.

Marked cell shrinkage in CANeoAnti-Pgp5 was indicative of cytoplasm fluid loss and other ionic alterations such as an increase in cytosolic Ca^{2+} concentration. We measured intracellular calcium concentration in trophozoites after 120 min of incubation with G418. Fig. 4 showed that non transfected trophozoites (CA) without G418 treatment displayed a basal calcium concentration of 40 nM; instead G418-treated trophozoites (CA-treated) displayed 165 nM, representing an increment of 312.5%. Measurement of intracellular calcium concentration of trophozoites transfected with the empty vector (CANeo) without G418 treatment displayed 70 nM. These results suggest that concentration differences between non-transfected and transfected trophozoites may be due the increase in the electrical conductivity during electroporation that promotes also cell permeability of internal trophozoite membranes, provoking calcium delivering from reservorious. Interestingly, CANeoAnti-Pgp5 trophozoites displayed 140 nM of intracellular calcium concentration, representing an increment of 100% of the calcium concentration from trophozoites transfected with the empty vector (CANeo). On the other hand, trophozoites from clone CANeoPgp5 showed similar calcium concentrations to CANeo, representing only a marginal increment of 14.2% (Fig. 4).

In other systems, imbalance of ionic concentrations alters membrane potential, which subsequently decreases $_{i}$pH levels (Kawasaki et al., 2009). Thus, we evaluated the changes in $_{i}$pH using DFCA.

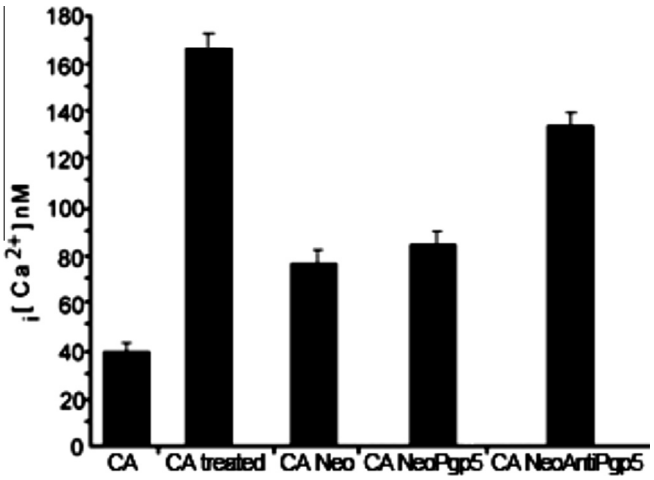

Fig. 4. Intracellular cytosolic Ca^{2+} concentration $_i(Ca^{2+})$ in trophozoites after G418 treatment. Ca^{2+} concentration was evaluated by fluorimetry using Fura-2/AM dye. Ca^{2+} measurements were performed for CA, CANeoPgp5 and CANeo-AntiPgp5 after treatment with G418 (10 μg/ml) for 12 h. CA and CANeo trophozoites incubated without G418 were included as internal controls.

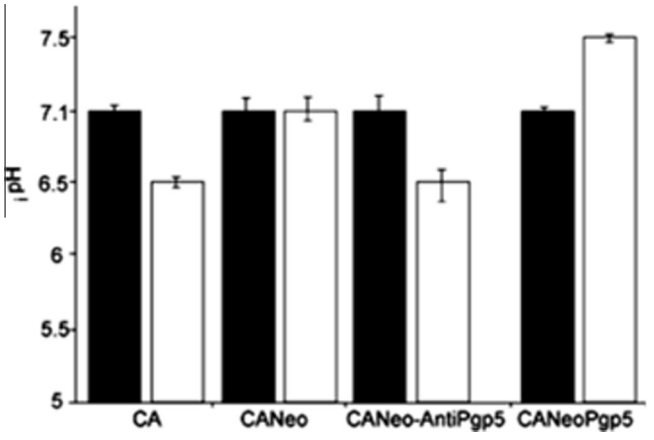

Fig. 5. Intracellular pH ($_i$pH) measurement in trophozoites before and after G418 treatment. $_i$pH was examined by using BCECF fluorescent dye in CA, CANeo, CANeoPgp5 and CANeoAnti-Pgp5 trophozoites before (solid bars) and after G418 treatment (empty bars).

Fig. 5 demonstrates that $_i$pH during CA clone growth without G418 antibiotic was 7.1; however, when trophozoites were cultured in the presence of G418, the $_i$pH decreased to 6.5. In concordance with the biochemical alterations previously presented, the $_i$pH of CANeoAnti-Pgp5 was also acidified ($_i$pH 6.7). In contrast, CANeoPgp5 trophozoites incubated in the presence of G418 that overexpressed P-glycoprotein had an alkalinized $_i$pH, from 7.1 to 7.4. As expected, also trophozoites transfected with pNeo (CANeo) incubated in the presence of G418 remained at a neutral $_i$pH (7.1).

4. Discussion

A growing body of evidence supports the occurrence of PCD in *E. histolytica*. A variety of different external stimuli including antibiotics (Villalba et al., 2011) as well as oxygen and nitric oxide species (Ghosh et al., 2010; Ramos et al., 2007) induced similar characteristics of PCD compared to those reported in other organisms. Although the final phenotype resembled apoptosis in multicellular organisms, several differences existed in the molecular pathways and time course of events. In unicellular organisms, it remains to be known how diverse extracellular signals, such as growth factor withdrawal, reactive species, heat shock and drug exposure, lead to the similar sequence of morphological and biochemical changes that define PCD. In *E. histolytica*, we previously found (Villalba et al., 2007a,b) that these alterations potentially occur in a specific sequence and include changes in cell volume, intracellular $_i$pH, ROS, K^+ and Ca^{2+} ions along with the putative activation of proteases to produce the nuclear condensation and DNA damage. Recently using AFLP's polymorphisms and real-time qRT-PCR, we identified *grainin 1*, *grainin 2*, *sir-2*, *40S*, *glutaminyl-t-RNA synthetase* and *saposin-like* genes probably involved in pro- and anti-apoptotic gene signaling pathways (Sánchez et al., 2010).

One hypothesis is that the changes in intracellular ionic equilibrium might be involved in regulating PCD because profound changes in cellular volume and pH appear to occur early in PCD (Barry et al., 1993).

Several studies reported that multidrug-resistant P-glycoproteins, which are located in the cellular plasma membrane, have been associated with drug transport (Bañuelos et al., 2002) and the regulation of cellular permeability (Valverde et al., 1996), while other reports also suggested that P-glycoproteins were associated with apoptosis (Robinson et al., 1997). In *E. histolytica*, we demonstrated that P-glycoprotein overexpression was correlated with an increase in drug export from the cell (Bañuelos et al., 2002). P-glycoprotein also induced trophozoite swelling and probably functioned as a chloride channel or a chloride channel regulator (Delgadillo et al., 2002).

The present study evaluated the effect of P-glycoprotein antisense interference in the PCD phenotype by a variety of independent measures. Two different constructs were employed, pNEOEhPgp5 containing the *EhPgP5* ORF and pNeoAnti-Pgp5 containing the *anti-EhPgp5* sequence. Even though antisense transfected trophozoites (CANeoAnti-Pgp5) also expressed the G418 resistance gene, no stable transfected trophozoites were obtained. Instead, trophozoites death along with the enhancement of biochemical and morphological characteristics of PCD were observed after 12 h of G418 incubation. Amoeba size diminished, while granularity increased. Importantly, the P-glycoprotein antisense interference enhanced DNA alterations induced by G418. While chromatin in G418-treated CA trophozoites appeared fragmented and displaced to one side of the amoeba nucleus, the ultrastructural architecture of CANeoAnti-Pgp5 trophozoites showed substantial differences: the nucleus was contracted, the nuclear membrane was disrupted, and chromatin was extensively fragmented. In contrast, nuclei from CANeo and CANeoPgp5 trophozoite clones treated with the antibiotic, kept their normal morphology and did not show ultrastructural DNA alterations. Previous reports in other systems suggested that besides the efflux pump function of PGP, it also appears to reduce apoptosis induced by drugs and other stressors at a variety of levels within death signaling pathways (Dudley, 1998; Fojo and Bates, 2003). Upon treatment with doxorubicin, P388/Dox cells (a doxorubicin drug-resistant P388 murine leukemia cell line) exhibit a reduction in DNA laddering, which is a characteristic of apoptosis (Ling et al., 1993). More recently, results from two different groups clarified the relationship between the expression of P-glycoprotein, apoptosis and drug resistance. Xiaohua et al., 2007 suggested that CIAPIN1 (cytokine-induced apoptosis inhibitor 1) could significantly up-regulate the expression of *MDR1* and *Bcl-2* and the inhibition of CIAPIN1 expression by RNA interference as well as the use of Pgp inhibitors sensitized cells to drugs. In contrast, overexpression of human *REIC/DKK-3* (reduced expression in immortalized cell) gene, resulted in the sensitization of multidrug-resistant breast cancer MCF7/ADR cells to doxorubicin decreasing the levels of P-glycoprotein and inducing apoptosis in multidrug-resistant cells (Kawasaki et al., 2009).

Typically during apoptosis, cell shrinkage is caused by the loss of cytoplasmic fluid and the denaturation of proteins (Huppertz et al., 1999), which produces characteristic biochemical features. One of the critical determinants of the cellular response to exogenous stimuli is cellular redox status. Intracellular generation of ROS causes an increase in the level of lipid peroxidation (Sen et al., 2004b) that causes an osmotic imbalance and an increase in intracellular calcium levels. In unicellular organisms, particularly in protozoan parasites, there is a dearth of knowledge about the importance of cytosolic cations in the apoptotic process. In *Leishmania donovani*, the formation of ROS inside *leishmania* cells by CTP-induction causes an increase in the levels of lipids peroxidation and cytosolic calcium (Sen et al., 2004a). In Eukaryotes, normal intracellular Ca^{2+} concentrations range at ~100 nM, 20,000-fold lower than 2 mM concentrations found in the extracellular medium (Peng et al., 2003). Elevation of cytosolic Ca^{2+} causes cellular damage and death through the disruption of cytoskeleton networks and the action of Ca^{2+}-stimulated catabolic enzymes, such as proteases, phospholipases, and endonucleases (Tagliarino et al., 2001).

In other systems, excessive free cytosolic calcium, due to the opening of Ca^{2+} ATPase channels, leads to uncoupling of mitochondrial oxidative phosphorylation and directs the cells to follow the executionary part of apoptosis (Jiang et al., 1994). Recently, studies were carried out to determine whether changes in intracellular Ca^{2+} levels correlated with the apoptosis increment in time and dose dependent manner. In *Toxoplasma gondii* nitric oxide donor (SNP) that induced apoptosis-like death, produced intracellular calcium increment from 113 nM, of non-treated parasites, to 372 nM of apoptotic induced organisms. In our study, we observed that intracellular Ca^{2+} concentration in CANeoPgp5 and CANeo trophozoites were within normal intracellular range (100 nM), even though cell permeability induced by the electric field during electroporation produced an increment of calcium, from 40 nM of non-transfected trophozoites to 70 nM of transfected ones. However, trophozoites expressing the antisense sequence displayed more than 100% of the basal Ca^{2+} concentrations, suggesting that calcium increment could be directly related to the induction of molecular signals that mark trophozoites to PCD. Our results are also in concordance with those reported by Tagliarino et al., 2001, in which DNA fragmentation, mitochondrial membrane depolarization, ATP loss and apoptotic proteolysis in MCF-7 cancer cells were a consequence of the intracellular Ca^{2+} increment over 100 nM. Using acid acetoxymethyl ester, an intracellular Ca^{2+} chelator, early increases in Ca^{2+} levels and apoptosis were blocked (Sen et al., 2004a). Sen and co-workers, also demonstrated in *L. donovani* that pre-treatment with anti-oxidants like BHT (butyrated hidroxy toluene), also decreased the calcium concentrations and the apoptotic manifestations, even though the calcium levels remained 20 nM higher than normal parasites. The activation of several signaling pathways and late apoptosis events, such as nuclear condensation, protease and endonuclease activation as well as DNA fragmentation were preceded by early biochemical events. Acidification is an important early event in the apoptotic cascade (Robinson et al., 1997). The human LR73 tumor cell line transfected with the MDR1 became alkaline and exhibited a delay in the apoptotic phenotype (Hoffman et al., 1996). Thus, the delay in morphological changes and DNA laddering was potentially due to altered pH homeostasis, which suggested another mechanism by which MDR1 protein overexpression increases the survivability of tumor cells (Robinson et al., 1997).

In concordance with several studies (Gottlieb et al., 1996; Pérez-Sala et al., 1995), our results strongly suggested that changes in intracellular ionic equilibrium is involved in regulating PCD in *E. histolytica* via key regulators of intracellular ion homeostasis, such as P-glycoproteins. Inhibition of *E. histolytica* PGP protein precipitated the onset of PCD induced by G418 antibiotic, while PGP overexpression prevented intracellular acidification and circumvented its apoptotic effect. Our results also potentially conveyed that PGP protein overexpression in *E. histolytica* confers resistance to other PCD inducers, *in vitro* and *in vivo*. Using an *in vivo* model in which physical interaction between amoebas and inflammatory cells was limited, we recently found that nitric oxide produced by inflammatory cells induces PCD in 86% of the trophozoite population; however, 14% of them were resistant to death (Villalba et al., 2011). In conclusion, the involvement of PGP in controlling the intracellular acidification blocking the global switch that inactivate cellular processes and the molecular mechanisms implicated in the destruction of the genome, represents a medullar role for PCD resistance. Our results represented the first evidence in parasites and other unicellular organisms of a specific molecule participating in the regulation of PCD pathways. PCD regulating molecules might be important for understanding the early events in host-parasite interactions that could be consequently involved with the initiation of the physiopathology of disease. Further studies might shed light on the relationship between signaling in the apoptotic cascade and altered intracellular ionic equilibrium observed in *E. histolytica* trophozoites.

Acknowledgments

This work was supported by CONACYT and SIP-IPN grants given to D.G.P.I. The authors gratefully acknowledge the collaboration from Dr. Mineko Shibayama's laboratory at CINVESTAV-IPN, especially the assistance of Angelica Silva-Olivares with transmission electronic microscopy. We thank Dr. Julio Cesar Carrero from Instituto de Biomedicas-UNAM and also to Francisco Javier Paz Bermudez, Chemical Pharmacobiology from CINVESTAV-IPN for kindly support. Finally, we also express our gratitude to Veronica Castillo for graphical design.

References

Ambudkar, S.V., Dey, S., Hrycyna, C.A., Ramachandra, M., Pastan, I., Gottesman, M.M., 1999. Biochemical, cellular, and pharmacological aspects of the multidrug transporter. Annu. Rev. Pharmacol. Toxicol. 39, 361–398.

Bañuelos, C., Orozco, E., Gómez, C., Gonzalez, A., Medel, O., Mendoza, L., Perez, D.G., 2002. Cellular location and function of the P-Glycoproteins (EhPgps) in *Entamoeba histolytica* multidrug-resistant trophozoites. Microb. Drug Resist. 8, 291–300.

Barry, M.A., Reynolds, J.E., Eastman, A., 1993. Etoposide-induced apoptosis in human HL-60 cells is associated with intracellular acidification. Cancer Res. 53, 2349–2357.

Borst, P., Evers, R., Kool, M., Wijnholds, J., 1999. The multidrug resistance protein family. Biochim. Biophys. Acta 1461, 347–357.

Chose, O., Nöel, C., Gerbod, D., Brenner, C., Viscogliosi, E., Roseto, A., 2002. A form of cell death with some features resembling apoptosis in the amitochondrial unicellular organism *Trichomonas vaginalis*. Exp. Cell Res. 276, 32–39.

Cordon-Cardo, C., O'Brien, J.P., Casals, D., Ritmman-Grauer, L., Biedler, J.L., Melamed, M.R., Bertino, J.L., 1989. Multidrug-resistance gene (P-glycoprotein) is expressed by endothelial cells at blood–brain barrier sites. Proc. Natl. Acad. Sci. USA 86, 695–698.

De Souza, E.M., Menna-Barreto, R., Araujo-Jorge, T.C., Kumar, A., Hu, Q., Boykin, D.W., Soeiro, M.N.C., 2006. Antiparasitic activity of aromatic diamidines is related to apoptosis-like death in *Trypanosoma cruzi*. Parasitology 133, 75–79.

Delgadillo, D.M., Pérez, D.G., Gómez, C., Ponce, A., Paz, F., Bañuelos, C., Mendoza, L., López, C., Orozco, E., 2002. The *Entamoeba histlytica EhPgp5* (MDR-like) protein induces swelling of the trophozoites and alters chloride dependent currents in *Xenopus laevis* oocytes. Microb. Drug Resist. 8, 15–26.

Diamond, L.S., Harlow, Cunick, C., 1978. A new medium for axenic cultivation of *Entamoeba histolytica* and other *Entamoeba*. Trans. R. Soc. Trop. Med. Hyg. 72, 431–432.

Drach, J., Gsur, A., Hamilton, G., Zhao, S., Angerler, J., Fiegl, M., Zojer, N., Raderer, M., Haberl, I., Andreeff, M., Huber, H., 1996. Involvement of P-glycoprotein in the transmembrane transport of interleukin 2(IL-2), IL-4, and interferon-gamma in normal human T lymphocytes. Blood 88, 1747–1754.

Dudley, L.J., 1998. Apotosis in LR73 cells is inhibited by overexpression of the multidrug resistance (MDR) protein. J. Undergrad. Sci. 3, 8.

Fojo, T., Bates, S., 2003. Strategies for reversing drug resistance. Oncogene 22, 7512–7523.

Ghosh, A.S., Dutta, S., Raha, S., 2010. Hydrogen peroxide-induced apoptosis-like cell death in *Entamoeba histolytica*. Parasitol. Int. 59, 166–172.
Gottesman, M.M., Pastan, I., 1993. Biochemistry of multidrug resistance mediated by the multidrug transporter. Annu. Rev. Biochem. 62, 385–427.
Gottlieb, R.A., Nordberg, J., Skowronski, E., Babior, B.M., 1996. Apoptosis induced in jurkat cells by several agents is preceded by intracellular acidification. Proc. Nat. Acad. Sci. 93, 654–658.
Grynkiewicz, G., Poenie, M., Tsien, R.Y., 1985. A new generation Ca^{2+} indicators with greatly improved fluorescence propieties. J. Biol.Chem. 260, 3440–3450.
Hanna, R.M., Dahniya, M.H., Badr, S.S., El-Betagy, A., 2000. Percutaneous catheter drainage in drug-resistant amoebic liver abscess. Trop. Med. Int. Health 5, 578–581.
Hawley, T., Hawley, R.G., 2004. Methodos in Molecular Biology. Flow Cytometry Protocols, 2nd ed. Totowa., N.J. Humana Press 45-64.
Hoffman, M.M., Wei, L.Y., Roepe, P.D., 1996. Are altered pHi and membrane potential in hu MDR 1 transfectants sufficient to cause MDR protein-mediated multidrug resistance? J. Gen. Physiol. 108, 295–313.
Holzmuller, P., Sereno, D., Cavaleyra, M., Mangot, I., Daulouede, S., Vincendeau, P., Lemesre, J.L., 2002. Nitric oxide-mediated proteasome-dependent oligonucleosomal DNA fragmentation in *Leishmania amazonensis* amastigotes. Infect. Immun. 70, 3727–3735.
Huppertz, B., Frank, H., Kaufmann, P., 1999. The apoptosis cascade-morphological and inmunohistochemical methods for its visualization. Anat. Embryol. 2000, 1–18.
Jiang, S., Chow, S.C., Nicotera, P., Raff, M.C., 1994. Intracellular Ca^{2+} signals activate apoptosis in thymocytes: studies using the Ca^{2+} ATPase inhibitor thapsigargin. Exp. Cell Res. 212, 84–92.
Jonstone, J.W., Ruefli, A.A., Smyth, M., 2000. Multiple physiological functions for multidrug transporter P-glycoprotein? Trends Biochem. Sci. 25, 1–6.
Kawasaki, K., Watanabe, M., Sakaguchi, M., Ogasawara, Y., Ochiai, K., Nasu, Y., Doihara, H., Kashiwakura, Y., Hun, N.-h., Date, H., 2009. REIC/Dkk-3 overexpression downregulates P-glycoprotein in multidrug-resistant MCF7/ADR cells and induces apoptosis in breast cancer. Cancer Gene Ther. 16, 65–72.
Ling, Y.H., Prieb, W., Pérez-Soler, R., 1993. Apoptosis induced by anthracycline antibiotics in P388 parents and multidrug-resistant cells. Cancer Res. 53 (8), 1845–1852.
Livak, K.J., Schmittgen, T.D., 2001. Analysis of relative gene expressión data using real-time quantitative PCR and 2 (Delta delta CT) method. Methods 25, 402–408.
Meisenholder, G.W., Martin, S.J., Green, D.R., Babior, B.M., Gottlieb, R.A., 1996. Events in apoptosis. Acidification is drowstream of protease activation and BCl-2 protection. J. Biol. Chem. 271, 16260–16262.
Nickel, R., Tannich, E., 1994. Transfection and transient expression of chloramphenicol acetyltransferase gene in the protozoan parasite *Entamoeba histolytica*. Proc. Natl. Acad. Sci. 91, 7095–7098.
Peng, B.W., Ling, J., Ling, J.Y., Jiang, M.S., Zhang, T., 2003. Exogenous nitric induces apoptosis in Toxoplasma gondii tachyzoites via a calcium signal transduction pathway. Parasitology 126, 541–550.
Pérez-Sala, D., Collado-Escobar, D., Mollinedo, F., 1995. Intracellular alkalinization suppresses lovastatin-induced apoptosis in HL-60 cells through the inactivation of a pH dependent endonuclease. J. Biol. Chem. 270, 6235–6242.
Perl, M., Chung, C.S., Ayala, A., 2005. Apoptosis. Crit. Care Med. 33, S526–S529.
Ramos, E., Olivos-García, A., Nequiz, M., Saavedra, E., Tello, E., Saralegui, A., Montfort, I., Tamayo Pérez, R., 2007. *Entameoba histolytica*: apoptosis induced *in vivo* by nitric oxide species. Exp. Parasitol. 116, 257–265.
Robinson, L.J., Roberts, W.K., Ling, T.T., Lamming, D., Stemberg, S.S., 1997. Human MDR1 protein overexpression delays the apoptotic cascade in hamster ovary fibroblasts. Biochemistry 36, 11169–11178.
Samarawickrema, N.A., Brown, D.M., Upcroft, J.A., Thammapalerd, N., Upcroft, P., 1997. Involvement of superoxide dismutase and pyruvate:ferredoxin oxidoreductase in mechanisms of metronidazole resistance in *Entamoeba histolytica*. J. Antimicrob. Chemother. 40, 833–840.
Sánchez, M.V., Medel, F.O., Villalba, M.J.D., Gómez, C., Pérez, I., 2010. *Entamoeba histolytica*: differential gene expression during programmed cell death and identification of early pro- and anti-apoptotic signals. Exp. Parasitol. 126, 497–505.
Sen, N., Das, B.B., Ganguly, A., Mukherjee, T., Bandyopadhyay, S., Majumder, H.K., 2004a. Camptothecin-induced imbalance in intracellular cation homeostasis regulates programmed cell death in unicellular hemoflagellate *Leishmania donovani*. J. Biol. Chem. 279, 52366–52375.
Sen, N., Das, B.B., Ganguly, A., Mukherjee, T., Tripathi, G., Bandyopadhyay, S., Rakshit, S., Sen, T., Majumder, H.K., 2004b. Camptothecin induced mitocondrial dysfunction leading to programmed cell death in unicellular hemoflagellate *Leishmania donovani*. Cell Death Differ. 11, 924–936.
Sharom, F.J., Yu, X., Doige, C.A., 1993. Functional reconstitution of drug transport and ATPase activity in proteoliposomes containing partially purified P-glycoprotein. J. Biol. Chem. 268 (32), 24192–24202.
Tagliarino, C., Pink, J.J., Dubyak, G.R., Nieminen, A.L., Boothman, D.A., 2001. Calcium is a key signaling molecule in β-lapachone-mediated cell death. J. Biol. Chem. 276, 19150–19159.
Tsai, S.H., Sun, N.K., Lu, H.P., Cheng, M.L., Chao, C.C.K., 2007. Involvement of reactive oxygen species in multidrug resistance of vincristine-selected lymphoblastoma. Cancer Sci. 98 (8), 1206–1214.
Valverde, M.A., Bond, T.D., Hardy, S.P., Taylor, J.C., Higgins, C., Altamirano, J., Alvarez-Leefmans, F.J., 1996. The multidrug resistance P-glycoprotein modulates cell regulatory volume decrease. EMBO J. 15 (17), 4460–4468.
Van Helvoort, A., Smith, A.J., Sprong, H., Fritzsche, I., Schinkel, A.H., Borst, P., van Meer, G., 1996. MDR1 P-glycoprotein is a lipid translocase of broad specificity, while MDR3 P-glycoprotein specifically translocates phosphatidylcholine. Cell 87, 507–517.
Villalba, J.D., Gómez, C., Medel, O., Sánchez, V., Carrero, J.C., Shibayama, M., Pérez, D.G., 2007a. Programmed cell death in *Entamoeba histolytica* induced by the aminoglycoside G418. Microbiology 153, 3852–3863.
Villalba, J.D., Rojas, R., Gómez, C., Shibayama, M., Carrero, J.C., Pérez, I.D.G., 2007b. Emetine produce *Entamoeba histolytica* death by inducing a programmed cell death. Am. J. Infect. Dis. 3, 110–114.
Villalba, J.D., Pérez, I.D.G., Serrano, L.J., Tsutsumi, V., Shibayama, M., 2011. In vivo programmed cell death of *Entameba histolytica* trophozoites in a hamster model of amoebic liver abscess. Microbiology 157, 1489–1499.
Wassmann, C., Hellberg, A., Tannich, E., Bruchhaus, I., 1999. Metronidazole resistance in the protozoan parasite *Entamoeba histolytica* is associated with increased expression of iron-containing superoxide dismutase and peroxiredoxin and decreased expression of ferredoxin 1 and flavin reductase. J. Biol. Chem. 274, 26051–26056.
World Health Organization, 1997. Weekly epidemiological record. 72, 97–100.
Xiaohua, L., Liu, H., Yunping, Z., Haifeng, J., Rui, F., Rui, D., Lin, X., Guanhong, L., Daiming, F., 2007. Anew apoptosis inhibitor, ClAPIN1 (Cytokine-induced apoptosis inhibitor 1) mediates multidrug resistance in leukemia cells by regulating MDR-1, BCl-2, and Bax. Biochem. Cell Biol. 85, 741–750.